Super-resolving interference without intensity-correlation measurement

De-Zhong Cao,[1,*] Bao-Long Xu,[1] Su-Heng Zhang,[2] and Kaige Wang[3,†]
[1]*Department of Physics, Yantai University, Yantai 264005, Shandong Province, China*
[2]*College of Physics Science & Technology, Hebei University, Baoding 071002, Hebei Province, China*
[3]*Applied Optics Beijing Area Major Laboratory, Department of Physics, Beijing Normal University, Beijing 100875, China*
(Received 17 March 2015; published 28 May 2015)

The high-order intensity correlation function of N-photon interference with thermal light observed in a recent experiment [S. Oppel, T. Büttner, P. Kok, and J. von Zanthier, Phys. Rev. Lett. **109**, 233603 (2012)] is analyzed. The terms in the expansion of the Nth-order correlation function are put into three groups. One group contributes a homogeneous background. Both of the other two contribute $(N-1)$-fold super-resolving fringes. In principle they correspond to coherent and incoherent superpositions of classical optical fields, respectively. Therefore similar super-resolving fringes can be obtained without intensity-correlation measurements. We report the experimental results of the coherent and incoherent super-resolving diffraction fringes, which are observed directly in the intensity distribution. The $N-1$ sources in both the coherent and incoherent cases are set in certain definite positions. In the coherent case, moreover, the phase difference between two adjacent source fields is π. The fringe visibility is unity in the incoherent case, while it decreases as N increases in the incoherent case.

DOI: 10.1103/PhysRevA.91.053853 PACS number(s): 42.25.Hz, 42.50.St

I. INTRODUCTION

Subwavelength interference fringes, which usually represent the shrinkage of the spatial spectrums of the objects, are one of the key characteristics for super-resolving optical imaging, optical lithography, and quantum metrology. In practice, the subwavelength diffraction pattern of an object can be obtained with NOON states [1,2] and with thermal light sources [3,4]. The physics behind this is that the de Broglie wavelength of the N-photon wave packet becomes $1/N$ of the single-photon wavelength [5]. Similar super-resolving interference fringes have been investigated with Nth harmonic generation [6], Fock state projection [7], time-reversal analysis [8], and multimode Gaussian states [9].

In previous subwavelength interference experiments, the N-photon correlation measurement systems are indispensable. In 2007, Thiel *et al.* [10] theoretically proposed a subwavelength N-photon interference scenario in which photons from N single-photon sources trigger N joint detectors. To obtain the super-resolving fringes, the N single-photon detectors are set jointly in a way that two detectors move in opposite directions, while the other detectors are located at certain definite positions. Recently, Oppel *et al.* [11] observed $(N-1)$-photon super-resolving fringes in an N-slit diffraction experiment with thermal light, where the N-photon correlation system contains one moving detector and $N-1$ fixed detectors.

However, such super-resolving fringes do not depend on N-photon correlation systems. Consider an ordinary N-slit diffraction experiment in which a laser beam, with complex field amplitude A_n and wavelength λ, illuminates N slits with slit spacing d. In the Frauhofer diffraction limit, the optical field in the detection plane is written as

$$\mathcal{E}(\delta,\delta_n) = A_n \sum_{m=1}^{N} \cos\left[(N+1-2m)\frac{\delta-\delta_n}{2}\right], \qquad (1)$$

where $\delta = 2\pi d \sin\theta/\lambda$, θ is the diffraction angle, and δ_n is the phase shift to describe the initial phase of the incident laser beam. Equation (1) is the sum of coherent superposed fields with a variety of spatial frequencies. The fundamental frequency term is $\cos[(\delta-\delta_n)/2]$. The highest frequency term $\cos[(N-1)(\delta-\delta_n)/2]$ stands for the $(N-1)$-fold super-resolving fringes. One can acquire the pure super-resolving fringes of the highest frequency, as long as the highest frequency terms dominate.

In this paper, we propose an N-slit diffraction experiment to directly obtain pure super-resolving fringes in intensity-distribution measurements. We make the highest frequency terms dominant by introducing coherent or incoherent $N-1$ sources. In both coherent and incoherent cases, the $(N-1)$ optical beams from the sources are arranged carefully to wash out the lower frequency terms in Eq. (1). Especially in the coherent case, the phase difference between the adjacent laser beams is π. The fringe visibility is unity in the coherent case, and $2/N$ in the incoherent case.

Our paper is organized as follows. The theoretical analysis of N-photon super-resolving fringes with thermal light is given in detail in Sec. II. We analyze the high-order intensity-correlation function of N-photon interference with thermal light in Ref. [11]. In the expansion of the Nth-order correlation function, we find two kinds of $(N-1)$-fold super-resolving fringes, which correspond to the coherent and incoherent superpositions of classical optical fields. In Sec. III we perform N-slit diffraction experiments in which $N-1$ coherent or incoherent beams along certain definite directions are employed. The super-resolving interference fringes are acquired directly in intensity observation, but not in intensity-correlation measurements. The fringe visibility is unity in the coherent case but decreases when the slit number increases in the incoherent case. The experimental results are in good agreement with our theoretical analysis. Section IV presents discussions and conclusions. The Appendix shows the calculations of the first-order and Nth-order correlation functions.

*dzcao@ytu.edu.cn
†wangkg@bnu.edu.cn

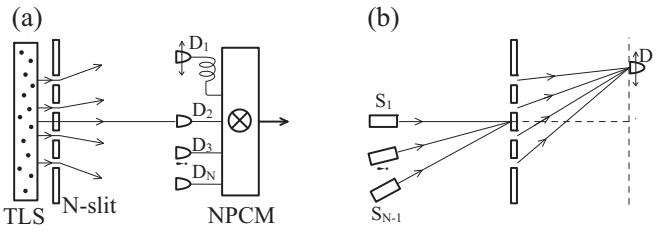

FIG. 1. (a) Setup of the N-photon super-resolving diffraction experiment performed by Oppel *et al.* [11] with thermal light. TLS represents the thermal light source. NPCM represents the N-photon correlation measurement. $D_1, D_2, \ldots, D_N$ are the N detectors. (b) The unfolded version of (a). The $N-1$ detectors ($D_2, D_3, \ldots, D_N$) are imagined to be $N-1$ sources ($S_1, S_2, \ldots, S_{N-1}$).

II. THERMAL LIGHT *N*th-ORDER CORRELATION FUNCTIONS AND SUPER-RESOLVING FRINGES

The schematic diagram of the N-photon super-resolving diffraction experiment performed by Oppel *et al.* [11] is replotted in Fig. 1(a). A beam of thermal light goes through N slits and then triggers N detectors. In the detection plane, one detector (D_1) scans and others ($D_2, \ldots, D_N$) are fixed in certain definite positions in which [11]

$$\delta_n = 2\pi d \sin\theta_n/\lambda = 2\pi(n-2)/(N-1), \tag{2}$$

where $n = 2, \ldots, N$. These positions in Eq. (2) are in accordance with the magic phase-shift settings proposed by Oppel, *et al.* [11].

The joint intensity-correlation measurement of the N detectors gives rise to the N-photon super-resolving diffraction patterns. In the far-field diffraction limit, by taking both the magic positions (2) and complete incoherence of the thermal light source into account, we calculate out the normalized first-order correlation functions as

$$g^{(1)}(\delta,\delta_n) = \frac{\langle E^*(\delta)E(\delta_n)\rangle}{\sqrt{\langle I(\delta)\rangle\langle I(\delta_n)\rangle}} = \frac{\sin[N(\delta-\delta_n)/2]}{N\sin[(\delta-\delta_n)/2]}, \tag{3}$$

$$g^{(1)}(\delta,\delta) = g^{(1)}(\delta_n,\delta_n) = 1, \tag{4}$$

$$g^{(1)}(\delta_m,\delta_n) = \frac{(-1)^{m-n}}{N} \quad (m \neq n), \tag{5}$$

where $\langle\cdots\rangle$ represents ensemble averaging, E is the detected field, $I(\delta) = E^*(\delta)E(\delta)$ is the instant intensity function, and $m,n = 2, \ldots, N$. According to the Gaussian moment theorem, one can expand the Nth-order correlation function

$$g^{(N)}(\delta,\delta_2,\ldots,\delta_N) = \frac{\langle I(\delta)I(\delta_2)\cdots I(\delta_N)\rangle}{\langle I(\delta)\rangle\langle I(\delta_2)\rangle\cdots\langle I(\delta_N)\rangle} \tag{6}$$

into terms of first-order correlation functions [12,13]

$$g^{(N)}(\delta,\delta_2,\ldots,\delta_N) = \sum_{N!}\mathcal{P}[g^{(1)}(\delta,\underline{\delta})g^{(1)}(\delta_2,\underline{\delta_2})\cdots g^{(1)}(\delta_N,\underline{\delta_N})], \tag{7}$$

where $\mathcal{P}$ represents the $N!$ possible permutations of the underlined fields. It is obvious in Eq. (7) that the spatial fringes come from terms of $g^{(1)}(\delta,\delta_n)$ [Eq. (3)]. We then put the $N!$ permutations in Eq. (7) into three groups. The first group contains $(N-1)!$ permutations which has the term of $g^{(1)}(\delta,\delta)$. The second group contains $(N-1)!$ permutations, each of which has terms of $|g^{(1)}(\delta,\delta_n)|^2$. The third group contains $(N-2)\times(N-1)!$ permutations, each of which has terms of $g^{(1)}(\delta,\delta_n)g^{(1)}(\delta_m,\delta)_{m\neq n}$. By summarizing the analysis above, we obtain the normalized high-order correlation function (see the Appendix)

$$g^{(N)}(\delta,\delta_2,\ldots,\delta_N) = A + B\left|\sum_{n=2}^{N}(-1)^n g^{(1)}(\delta,\delta_n)\right|^2 + C\sum_{n=2}^{N}|g^{(1)}(\delta,\delta_n)|^2. \tag{8}$$

The three coefficients are

$$A = \sum_{k=0}^{N-1}\frac{!k}{N^k}C_{N-1}^k, \tag{9}$$

$$B = \sum_{j=0}^{N-3}\frac{N^{-j}(N-3)!}{(N-3-j)!}\sum_{k=0}^{N-3-j}C_{N-3-j}^k\frac{!k}{N^{k+1}}, \tag{10}$$

$$C = \sum_{k=0}^{N-2}\frac{!k}{N^k}C_{N-2}^k - B, \tag{11}$$

respectively, where $C_M^k = \frac{M!}{k!(M-k)!}$, and $!k = k!\sum_{j=0}^{k}\frac{(-1)^j}{j!}$ is the derangement number [14].

In the right side of Eq. (8), the first term contributes a homogeneous background. Both of the last two terms contribute super-resolving fringes. Specifically, by substituting Eq. (3) into the last two terms of Eq. (8), we obtain

$$\left|\sum_{n=2}^{N}(-1)^n g^{(1)}(\delta,\delta_n)\right|^2 = 2(N-1)^2\frac{1+\cos[(N-1)\delta]}{N^2}, \tag{12}$$

$$\sum_{n=2}^{N}|g^{(1)}(\delta,\delta_n)|^2 = \frac{N-1}{N}\left[1+\frac{2}{N}\cos(N-1)\delta\right], \tag{13}$$

both of which manifest $(N-1)$-fold super-resolving fringes. It is obvious that Eq. (12) represents the coherent superposition of $N-1$ correlated fields. While Eq. (13) represents the incoherent superposition of $N-1$ correlated fields. The two kinds of super-resolving fringes can be obtained in intensity detection, as shown in the next section.

We further substitute Eqs. (12) and (13) into Eq. (8) and find the maximum and minimum values of $g^{(N)}$ as

$$g_{\max}^{(N)} = A + \frac{4(N-1)^2}{N^2}B + \frac{N-1}{N}\frac{N+2}{N}C, \tag{14}$$

$$g_{\min}^{(N)} = A + \frac{N-1}{N}\frac{N-2}{N}C, \tag{15}$$

respectively. So in the thermal light Nth-order correlation function (8), the visibility of the super-resolving

fringes is

$$V_0(N) = \frac{2}{N^2}\frac{(N-1)^2B + (N-1)C}{A + 2(\frac{N-1}{N})^2 B + \frac{N-1}{N}C}, \tag{16}$$

which decreases from $V_0(2) = 1/3$.

Since the thermal light source can be regarded as a conjugate mirror in high-order intensity-correlation functions [15], we unfold the configuration of the experimental setup as shown in Fig. 1(b). The $N-1$ detectors (D_2, D_3, ..., D_N) are imagined to be $N-1$ sources (S_1, S_2, ..., S_{N-1}), and the thermal light source (TLS) is omitted. The thermal light correlation in the experiment can become comprehensible as follows. The light beams from the $N-1$ fixed sources (S_1, S_2, ..., S_{N-1}) go back to the thermal source plane, then go forth through the N slits, and finally are registered by the moving detector D.

What we should emphasize is that the super-resolving $(N-1)$-fold interference fringes can be obtained just in the intensity distribution itself (not in the intensity correlation). In other words, the super-resolving $(N-1)$-fold fringes can be obtained in single-photon N-slit diffraction experiments, however, using a set of carefully arranged optical beams as the source configurations. Let us reexamine the forms of Eqs. (12) and (13). The former, which is the modulus square of the summation of $N-1$ parts, corresponds to coherent superposition of $N-1$ correlated fields. While the latter, which is the summation of the modulus squares of $N-1$ correlated parts, corresponds to incoherent superposition. These suggest that there are at least two methods for obtaining $(N-1)$-fold super-resolving fringes without intensity-correlation measurements.

III. COHERENT AND INCOHERENT SUPER-RESOLVING FRINGES IN INTENSITY DISTRIBUTION

We consider the N-slit interference experiment in which the $N-1$ beams from the optical source illuminate the N slits. According to Eq. (1), the total field in the detection plane is $E(\delta) = \sum_{n=2}^{N} \mathcal{E}(\delta,\delta_n)$. Owing to the fact that $\mathcal{E}(\delta,\delta_n) = NA_n g^{(1)}(\delta,\delta_n)$, we write the intensity distribution function in the detection plane as

$$\langle I(\delta)\rangle = N^2 \sum_{m,n=2}^{N} \langle A_m^* A_n\rangle g^{(1)}(\delta,\delta_m) g^{(1)}(\delta,\delta_n), \tag{17}$$

where the real functions $g^{(1)}(\delta,\delta_m)$ are considered. The complex amplitude correlation term $\langle A_m^* A_n\rangle$ of course plays an important role in obtaining super-resolving fringes. According to the last two terms in the right side of Eq. (8), we consider two kinds of illuminations, the coherent case and incoherent case, discussed as follows. Moreover we assume all the beam powers are equal, i.e., $\langle A_n^* A_n\rangle = I_0$, where I_0 is a constant, $n = 2, \ldots, N$.

A. Coherent case

In coherent illumination, the $N-1$ source beams have certain definite initial phases. By comparing Eqs. (12) and (17), we first set the directions of the $N-1$ coherent beams to meet the magic phase shifts (2). Second, we set the initial phase difference between any two adjacent beams to be π, so that the complex amplitude can be written as

$$A_n = \sqrt{I_0}\exp(in\pi) = (-1)^n\sqrt{I_0}, \tag{18}$$

where $n = 2, \ldots, N$. After some algebra, we obtain the detected field as

$$E(\delta) = 2(N-1)\sqrt{I_0}\cos[(N-1)\delta/2]. \tag{19}$$

The intensity-distribution function, which is the modulus square of Eq. (19), is proportional to Eq. (12). We should note that the visibility of the diffraction pattern is $V_1 \equiv 1$.

B. Incoherent case

In the incoherent case, the source beams have completely random phases so that

$$\langle A_m^* A_n\rangle_{m\neq n} = 0. \tag{20}$$

By considering the magic phase-shift settings (2) and the incoherent complex amplitude correlations (20), we obtain the intensity distribution function (17) as

$$I_2(\delta) = N(N-1)I_0\left[1 + \frac{2}{N}\cos(N-1)\delta\right]. \tag{21}$$

The visibility of the diffraction pattern is $V_2(N) = 2/N$.

Figure 2 shows the fringe visibility functions V_0, V_1, and V_2. As the correlation number N (which is also the slit number) increases, the value of V_0 decreases from 1/3. The coherent fringe visibility without intensity correlation V_1 always keeps its value of unity. While the value of V_2 decreases from unity. Both V_0 and V_2 tend to zero for very large N. It is interesting that the visibility value of V_2 is very close to that of V_0 at $N = 9$.

As a result, the fringe spaces in both Eqs. (19) and (21) are equal to $1/(N-1)$ of that in the ordinary N-slit interference experiment. The coherent sources can be acquired with $N-1$ well-arranged correlated laser beams. The initial phase difference between two adjacent beams is π. While the incoherent correlated sources can be acquired by using, for example, $N-1$ independent sources. All the correlated sources in both coherent and incoherent cases are located at certain definite positions as shown in Eq. (2).

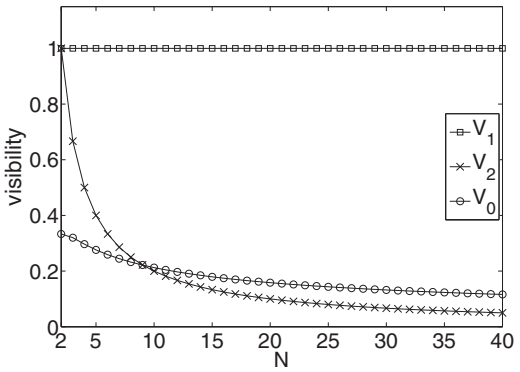

FIG. 2. Visibility functions vs N. The lines with circles, squares, and crosses are the visibility values for V_0, V_1, and V_2, respectively.

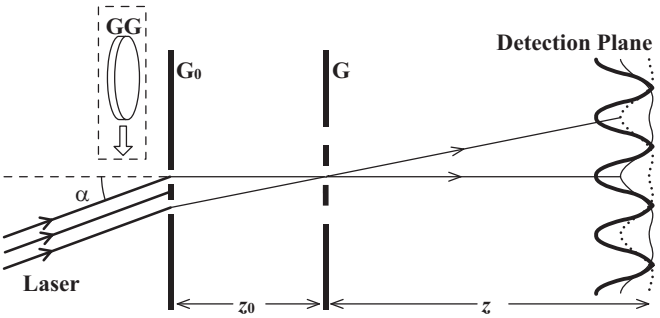

FIG. 3. Experimental setup of super-resolving fringes without intensity correlation. The laser beam gets through $N-1$ slits (G_0) and then N slits (G) in succession, and finally is detected by a CCD in the detection plane. GG is a ground glass plate, which is just used in the incoherent case. The slit spacing is $d_0 = 0.821$ mm for grating G_0, and $d = 0.197$ mm for grating G.

C. Experimental results

Figure 3 depicts the diagram of the experimental setup to observe coherent and incoherent super-resolving interference fringes without intensity correlation. The $(N-1)$ sources are composed of an optical beam and $N-1$ slits (G_0). The source beams go across the N slits (G), and then they are detected by a charge coupled device (CCD) in the detection plane.

In the case of coherent illumination, more precisely, the incident laser beam is projected onto G_0 at a certain angle α. This makes an initial phase difference $2\pi d_0 \sin\alpha/\lambda$ between the optical fields at two adjacent slits of G_0. Therefore, the initial phase difference π between any two adjacent beams in Eq. (18) can be met by setting the incident angle α as

$$\sin\alpha = (m + 1/2)\frac{\lambda}{d_0}, \tag{22}$$

where $m = 0, \pm1, \pm2, \ldots$, and d_0 is the slit spacing of grating G_0. To meet the magic phase-shift settings (2), the distance between the two gratings is

$$z_0 = (N-1)d_0 d/\lambda, \tag{23}$$

where d is the slit spacing of grating G. The coherent super-resolving interference fringes can be directly read out from the CCD signals.

To imitate the incoherent case, we insert a rotating ground glass plate (GG) between the laser source and G_0, and thus form $(N-1)$ pseudoindependent sources. The incoherent super-resolving fringes, however, can be obtained through averaging a certain number of CCD frames.

In the experiment, the laser wavelength is $\lambda = 650$ nm. The slit spacing is $d_0 = 0.821$ mm for grating G_0, and $d = 0.197$mm for grating G. According to Eq. (23) we have $z_0 = (N-1) \times 248.8$ mm. The distance from grating G to the detection plane (CCD) is $z = 547.0$ mm. Particularly, the slant angle of the incident beam in the coherent case is about $\alpha = 1.792 \times 10^{-3}$ rad, which meets Eq. (22). We note that $\delta = 2\pi dx/(\lambda z)$.

The experimental results are shown in Fig. 4. The slit number of G is $N = 2$ in Figs. 4(a) and 4(b), $N = 3$ in Figs. 4(c) and 4(d), and $N = 4$ in Figs. 4(e) and 4(f). In Figs. 4(a), 4(c), and 4(e), the circles indicate the coherent

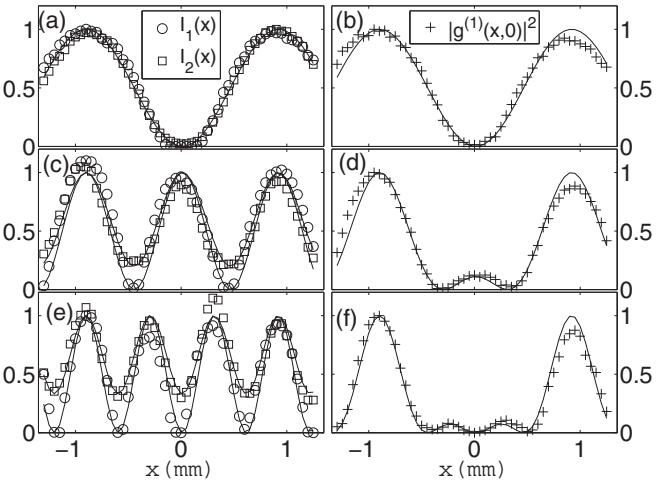

FIG. 4. Experimental results of $(N-1)$-fold super-resolving fringes (a), (c), and (e); and ordinary N-slit interference fringes (b), (d), and (f). We set $N = 2$ in (a) and (b), $N = 3$ in (c) and (d), and $N = 4$ in (e) and (f). The circles, squares, and pluses are the normalized I_1, I_2, and $|g^{(1)}(x,0)|^2$, respectively. The solid lines are the theoretical curves.

$(N-1)$-fold super-resolving fringes (I_1), which are obtained from one CCD shot. The squares indicate the incoherent $(N-1)$-fold super-resolving fringes (I_2), which are obtained by averaging 2 000 CCD frames. In contrast, the pluses in Figs. 4(b), 4(d), and 4(f) are the experimental data for ordinary N-slit interference fringes $[|g^{(1)}(\delta,0)|^2]$ illuminated by a single laser beam. Each experimental fringe is normalized with its maximum. All the solid lines in Fig. 4 are the theoretical curves.

Specifically, Fig. 4(a) shows the ordinary two-slit interference fringes with coherent (circles) and incoherent (squares) point sources. Their visibility values are close ($V_1 = 1.0$ and $V_2 = 0.955$), reflecting the spatial coherence of the sources. Figure 4(c) shows the coherent and incoherent two-fold super-resolving diffraction fringes. Their visibility values are $V_1 = 0.975$ and $V_2 = 0.622$, respectively. Figure 4(e) shows the coherent and incoherent three-fold super-resolving diffraction fringes. Their visibility values are $V_1 = 0.978$ and $V_2 = 0.496$, respectively. It is obvious that the visibility retains in the coherent case, and decreases in the incoherent case as slit number N increases.

The ordinary N-slit interference fringes, which are obtained by injecting a single coherent beam into the N slits, are shown in Figs. 4(b), 4(d), and 4(f). The fringe visibility values are $V = 0.970$, 0.966, and 0.961, respectively.

IV. DISCUSSIONS AND CONCLUSIONS

In summary, we in detail analyzed the Nth-order correlation functions in a multiphoton super-resolving interference experiment with thermal light. We put the expanded terms of the Nth-order correlation function into three categories. One contributes a background. The other two contribute the super-resolving fringes. However, the last two categories correspond to coherent and incoherent superpositions of correlated fields. So the super-resolving fringes can be obtained without multi-

photon processes or intensity-correlation measurements. We experimentally demonstrated $(N-1)$-fold super-resolving diffraction patterns in just intensity detection by projecting $N-1$ coherent and incoherent beams onto N slits. In the case of coherent illumination, the fringe visibility is unity. While for incoherent illumination, the fringe visibility decreases as the slit number increases.

The super-resolving N-fold fringes are just derived from the coherent and incoherent superpositions of $N-1$ correlated fields. Nevertheless, these superpositions are not the shrunk spatial spectra of the objects. Therefore there is a long way from such super-resolving fringes to super-resolving imaging.

ACKNOWLEDGMENTS

This work was supported by the National Natural Science Foundation of China, Projects No. 11047004, No. 11204062, and No. 11174038. S.H.Z. acknowledges the support of the Youth Foundation of Hebei Educational Committee (QN2014086).

APPENDIX: ARBITRARY *N*TH-ORDER CORRELATION FUNCTIONS WITH THERMAL LIGHT

First-order correlation function. We designate the Cartesian coordinates of the source plane and the detection plane in Fig. 1 by x_s and x, respectively. The optical field in the detection plane is written as

$$E(x)=\int E_s(x_s)T(x_s)h(x_s,x)dx_s, \tag{A1}$$

where E_s is the source field, the impulse response function is

$$h(x_s,x)=\frac{1}{\sqrt{i\lambda z}}\exp\left[i2\pi z+i\frac{\pi}{\lambda z}(x-x_s)^2\right] \tag{A2}$$

in Fresnel diffraction limit, and T is the source profile which is composed of N slits,

$$T(x_s)=\sum_{n=1}^{N}\delta\left[x_s-\left(n-\frac{N+1}{2}\right)d\right], \tag{A3}$$

where d is the slit distance. Taking into account the complete incoherence of the thermal light source $\langle E_s^*(x_s)E_s(x_s')\rangle = I_s\delta(x_s-x_s')$ and Eqs. (A1) and (A2), we obtain the field cross-correlation function

$$\langle E^*(x)E(x')\rangle=\frac{I_s}{\lambda z}\int|T(x_s)|^2\exp\left[i2\pi\frac{x-x'}{\lambda z}x_s\right]dx_s. \tag{A4}$$

Substituting Eq. (A3) into the above equation we obtain

$$\langle E^*(x)E(x')\rangle=\frac{I_s}{\lambda z}\frac{\sin\left[\frac{N\pi d}{\lambda z}(x-x')\right]}{\sin\left[\frac{\pi d}{\lambda z}(x-x')\right]}. \tag{A5}$$

Equation (3) is the normalized form of (A5) by defining $\delta=\frac{2\pi dx}{\lambda z}$ and $\delta_n=\frac{2\pi dx_n}{\lambda z}$.

Normalized high-order correlation function. In the N-photon detection system in Fig. 1, one detector scans and other detectors are fixed in the detection plane. What the joint-detection system gives is the Nth-order correlation function as shown in Eq. (7). Consequently, this can be regarded as a permutation problem in which the positions of the negative fields (E^*) are fixed, while the positions of the positive fields (E) permute randomly. There are $N!$ possible permutations. Each of them in Eq. (7) is the product of N first-order correlation functions. Only the permutations, which contain terms of $g^{(1)}(\delta,\delta_n)$ and $g^{(1)}(\delta_m,\delta)$, directly contribute to the super-resolving fringes.

We then put all the $N!$ permutations into three groups. The first group is composed of permutations, each of which contains $g^{(1)}(\delta,\delta)$. This group contributes a homogeneous background. In the second group, each permutation is concerned with $|g^{(1)}(\delta,\delta_n)|^2$. In the third group, each permutation contains $g^{(1)}(\delta,\delta_n)$ and $g^{(1)}(\delta_m,\delta)$, in which $n\neq m$. The last two groups contribute super-resolving fringes.

As shown above, one or two first-order correlation functions are determined in all permutations in the three groups. The underlined variables of the other first-order correlation functions in each permutation can permute freely. To calculate out the sum of all the permutations, we call $g^{(1)}(\delta,\delta)$ and $g^{(1)}(\delta_n,\delta_n)$ in Eq. (3) the ordered terms, and $g^{(1)}(\delta_m,\delta_n)_{m\neq n}$ in Eq. (4) the deranged terms. According to Eqs. (3) and (4), the value of each permutation is governed by the deranged terms.

According to combinatorial mathematics, the combination of the deranged terms forms a derangement, which is a permutation in which no element appears in its original position. The number of derangements is [14]

$$!k=k!\sum_{j=0}^{k}\frac{(-1)^j}{j!} \tag{A6}$$

for the case that all of the k elements in a set change their initial places.

In each permutation in the first group, the ordered term $g^{(1)}(\delta,\delta)=1$ is set. There are $(N-1)!$ permutations for other $N-1$ first-order correlation functions. The sum of all the elements in the first group is

$$\sum_{k=0}^{N-1}\frac{!k}{N^k}C_{N-1}^{k}, \tag{A7}$$

where $C_M^k=\frac{M!}{k!(M-k)!}$. In the summation of Eq. (A7), there are k deranged terms and $N-1-k$ ordered terms. We note that $\sum_{k=0}^{N-1}C_{N-1}^{k}\,!k=(N-1)!$, which is the number of permutations in the first group.

In each permutation in the second group, two terms, $g^{(1)}(\delta,\delta_n)$ and $g^{(1)}(\delta_n,\delta)$ $(n=2,\ldots N)$, are set in the product of N first-order correlations. Once n is chosen, other $N-2$ first-order correlation functions have $(N-2)!$ possible permutations. According to the derangement theory, we sum up the second group and obtain

$$\sum_{k=0}^{N-2}\frac{!k}{N^k}C_{N-2}^{k}\sum_{n=2}^{N}|g^{(1)}(\delta,\delta_n)|^2. \tag{A8}$$

We note that $\sum_{k=0}^{N-2}C_{N-2}^{k}\,!k\sum_{n=2}^{N}1=(N-1)!$, which is the number of permutations in the second group.

In the last group, two different terms $g^{(1)}(\delta,\delta_n)g^{(1)}(\delta_m,\delta)$ $(m\neq n)$ in each permutation are preset. In the other $N-2$ terms, the negative fields $E^*(\delta_n)$ and $E^*(\delta)$ are absent, and

the positive fields $E(\delta_m)$ and $E(\delta)$ are absent. Therefore the maximum number of ordered terms is $N-3$. The sum of all the elements in the third group is

$$\sum_{j=0}^{N-3}\frac{N^{-j}(N-3)!}{(N-3-j)!}\sum_{k=0}^{N-3-j}C_{N-3-j}^{k}\frac{!k}{N^k}\times\sum_{m\neq n=2}^{N}\frac{(-1)^{n-m}}{N}g^{(1)}(\delta,\delta_n)g^{(1)}(\delta_m,\delta). \tag{A9}$$

We note that $\sum_{j=0}^{N-3}\frac{(N-3)!}{(N-3-j)!}\sum_{k=0}^{N-3-j}C_{N-3-j}^{k}\,!k\sum_{m\neq n=2}^{N}1=(N-2)(N-1)!$, which is the number of permutations in the third group.

The expression of the Nth-order correlation function with thermal light can be obtained by considering Eqs. (A7)–(A9). However, the last summation in Eq. (A9) is not complete, $m\neq n$. The lack can be supplied by combining Eqs. (A8) and (A9). We then write the normalized Nth-order correlation function as

$$g^{(N)}(\delta,\delta_2,\ldots,\delta_N)=A+B\left|\sum_{n=2}^{N}(-1)^n g^{(1)}(\delta,\delta_n)\right|^2+C\sum_{n=2}^{N}|g^{(1)}(\delta,\delta_n)|^2, \tag{A10}$$

where the coefficients are

$$A=\sum_{k=0}^{N-1}\frac{!k}{N^k}C_{N-1}^{k}, \tag{A11}$$

$$B=\sum_{j=0}^{N-3}\frac{N^{-j}(N-3)!}{(N-3-j)!}\sum_{k=0}^{N-3-j}C_{N-3-j}^{k}\frac{!k}{N^{k+1}}, \tag{A12}$$

$$C=\sum_{k=0}^{N-2}\frac{!k}{N^k}C_{N-2}^{k}-B. \tag{A13}$$

Some examples. In the case $N=2$, the three coefficients are $A=1$, $B=0$, and $C=1$. And the second-order correlation function is

$$g^{(2)}(\delta,\delta_2)=1+|g^{(1)}(\delta,\delta_2)|^2=\tfrac{3}{2}\left[1+\tfrac{1}{3}\cos\delta\right]. \tag{A14}$$

The visibility is $V=1/3$.

In the case $N=3$, the three coefficients are $A=\frac{10}{9}$, $B=\frac{1}{3}$, and $C=\frac{2}{3}$. And the third-order correlation function is

$$g^{(N)}(\delta,\delta_2,\delta_3)=\frac{50}{27}\left[1+\frac{8}{25}\cos 2\delta\right].$$

The visibility is $V=0.32$.

[1] A. N. Boto, P. Kok, D. S. Abrams, S. L. Braunstein, C. P. Williams, and J. P. Dowling, Phys. Rev. Lett. **85**, 2733 (2000).

[2] I. Vidal, E. J. S. Fonseca, and J. M. Hickmann, Phys. Rev. A **82**, 043827 (2010).

[3] J. Xiong, D. Z. Cao, F. Huang, H. G. Li, X. J. Sun, and K. Wang, Phys. Rev. Lett. **94**, 173601 (2005).

[4] F. Guerrieri, L. Maccone, F. N. C. Wong, J. H. Shapiro, S. Tisa, and F. Zappa, Phys. Rev. Lett. **105**, 163602 (2010).

[5] J. Jacobson, G. Björk, I. Chuang, and Y. Yamamoto, Phys. Rev. Lett. **74**, 4835 (1995).

[6] S. Bentley and R. Boyd, Opt. Express **12**, 5735 (2004).

[7] G. Khoury, H. S. Eisenberg, E. J. S. Fonseca, and D. Bouwmeester, Phys. Rev. Lett. **96**, 203601 (2006).

[8] K. J. Resch, K. L. Pregnell, R. Prevedel, A. Gilchrist, G. J. Pryde, J. L. O'Brien, and A. G. White, Phys. Rev. Lett. **98**, 223601 (2007).

[9] S. Shabbir, M. Swillo, and G. Björk, Phys. Rev. A **87**, 053821 (2013).

[10] C. Thiel, T. Bastin, J. Martin, E. Solano, J. von Zanthier, and G. S. Agarwal, Phys. Rev. Lett. **99**, 133603 (2007).

[11] S. Oppel, T. Büttner, P. Kok, and J. von Zanthier, Phys. Rev. Lett. **109**, 233603 (2012).

[12] L. Mandel and E. Wolf, *Optical Coherence and Quantum Optics* (Cambridge University, Cambridge, England, 1995).

[13] D. Z. Cao, J. Xiong, S. H. Zhang, L. F. Lin, L. Gao, and K. Wang, Appl. Phys. Lett. **92**, 201102 (2008).

[14] R. A. Brualdi, *Introductory Combinatorics*, 5th ed. (Pearson Education Asia Limited and China Machine Press, Beijing, 2009).

[15] D. Z. Cao, J. Xiong, and K. Wang, Phys. Rev. A **71**, 013801 (2005).